Published in final edited form as:
Clin Exp Pharmacol Physiol. 2008 October ; 35(10): 1156–1163. doi:10.1111/j.1440-1681.2008.04984.x.

The vascular dysfunction in the α-galactosidase A knockout mouse is an endothelial cell, plasma membrane-based defect

James L Park[1], **Steven E Whitesall**[2], **Louis G D'Alecy**[2,3,4], **Liming Shu**[1], and **James A Shayman**[1]

[1]Division of Nephrology, Department of Internal Medicine, University of Michigan Medical Center, Ann Arbor, MI, USA

[2]Department of Molecular and Integrative Physiology, University of Michigan Medical School, Ann Arbor, Michigan, USA

[3]Department of Surgery, University of Michigan Medical School, Ann Arbor, Michigan, USA

[4]Department of Surgery, William Beaumont Hospital, Royal Oak, Michigan, USA

Summary

1. Fabry disease results from an X-linked mutation in the lysosomal α-galactosidase A (*Gla*). Defective *Gla* results in multi-organ accumulation of neutral glycosphingolipids (GSLs), especially in the vascular endothelium, the major accumulating GSL being globotriaosylceramide (Gb3). Excessive endothelial Gb3 accumulation is associated with increased thrombosis, atherogenesis, and endothelial dysfunction. The mechanism(s) by which endothelial dysfunction occurs, however, is unclear. The purpose of this study was to further characterize the vasculopathy associated with a murine model of Fabry disease.

2. Vascular reactivity was performed in vessels from wildtype (*Gla* +/0) and *Gla* knockout (*Gla* -/0) mice. Conscious blood pressure and heart rate were measured in the *Gla* +/0 and *Gla* -/0 mice by telemetry.

3. The present study demonstrates that vascular smooth muscle (VSM) contractions were blunted in the *Gla* -/0 mice to phenylephrine and serotonin, but not to U46619. Endothelium-dependent contraction and receptor-mediated endothelium-dependent relaxation to acetylcholine were significantly attenuated in vessels from *Gla* -/0 mice. However, receptor-independent endothelium-dependent relaxation to the calcium ionophore, ionomycin, remained intact in vessels from *Gla* -/0 mice. Furthermore, VSM reactivity was normal in the aortas from *Gla* -/0 mice in the absence of endothelium. These changes in vascular function were observed without changes in whole-animal blood pressure or heart rate.

4. These results suggest that the vasculopathy associated with Fabry disease is localized to the endothelium despite the accumulation of GSLs throughout the vasculature.

Keywords

α-galactosidase A; endothelium; Fabry disease; globotriaosylceramide

Address for correspondence: James A. Shayman, MD, University of Michigan, 1560 MSRB2, 1150 W. Medical Center Drive, Ann Arbor, MI 48109-5676, Phone: (734) 763-0992, Facsimile: (734) 763-0982, jshayman@umich.edu.

Disclosures: None

Introduction

Fabry disease, a rare lysosomal storage disorder, results from a deficiency in the lysosomal hydrolase, α-galactosidase A (*Gla*) (1,2). The multi-organ accumulation of neutral glycosphingolipids (GSLs) with α-galactosyl linkages, primarily globotriaosylceramide (Gb3), is the consequence of deficient lysosomal *Gla* activity (3,4). Because the disease is a recessive, X-linked disorder, hemizygous males are more severely affected by the disease, and premature mortality is the result of the development of renal insufficiency and end-stage renal disease, as well as cardiovascular and cerebrovascular complications (5,6).

The basis for these cardio- and cerebrovascular complications associated with Fabry disease may be derived, in part, from endothelial dysfunction associated with Gb3 accumulation in vascular endothelium. To date, previous studies have demonstrated Gb3 accumulation in both vascular smooth muscle and endothelium in the vasculature of Gla knockout (Gla -/0) mice (7,8), a murine model for Fabry disease (9). The increased vascular Gb3 accumulation has been associated with an increased propensity for thrombosis (7,10), as well as increased atherogenesis (11), both of which are associated with endothelial dysfunction.

Excess endothelial Gb3 is believed to contribute to endothelial dysfunction associated with Fabry disease (12), and Heare and colleagues demonstrated that blunted endothelium-dependent relaxation is associated with increased vascular Gb3 accumulation in older (19 months old) *Gla* -/0 mice (13). The purpose of this study was to further characterize the vasculopathy associated with a murine model of Fabry disease. Reactivity was performed in isolated vessels from wildtype (*Gla* +/0) and *Gla* -/0 mice. Our results demonstrate that vascular contractility to phenylephrine and serotonin, but not to U46619, were blunted. Endothelium-dependent contraction and relaxation to acetylcholine also were attenuated, while receptor-independent endothelium-dependent relaxation remained intact in *Gla* -/0 mice. Furthermore, vascular reactivity was normalized in aortas from *Gla* -/0 mice after endothelium removal. These changes in vascular function were evident despite insignificant changes in consciously-measured blood pressure and heart rate. These results suggest that vasculopathy in this model of Fabry disease is localized to the endothelium despite the accumulation of GSLs throughout the vasculature. More importantly, these observations suggest that the endothelial defect may stem from excess GSLs affecting receptor coupling, thereby extending our understanding of how excess endothelial GSL accumulation may have a functional impact on vascular function and pharmacology.

Methods

Mice

Male C57Bl/6 mice (wildtype; 12 - 20 weeks old) were from Charles River (Wilmington, MA) or Jackson Laboratories (Bar Harbor, ME). Male *Gla* knockout (*Gla* -/0) mice (9) were bred from mice provided by Drs. Ashok Kulkarni and Roscoe Brady (National Institutes of Health, Bethesda, MD). These mice were backcrossed at least five generations to the C57Bl/6 strain. All mice were maintained on normal chow in specific pathogen-free facilities.

The procedures performed in mice were in accordance with guidelines of the University of Michigan Committee on the use and care of animals. The University of Michigan Unit for Laboratory Animal Medicine provided veterinary care. The University of Michigan is accredited by the American Association of laboratory Animal Care. The animal care and use program conformed to the standards in “The Guide for the Care and Use of laboratory Animals,” Department of Health, Education, and Welfare Publication No. (NIH) 86-23.

Direct Blood Pressure and Heart Rate Measurements with Radiotelemetry

Blood pressure and heart rate were measured in wildtype and *Gla* -/0 mice as previously described (14). Briefly, the left common carotid artery was cannulated with the catheter of a telemetric blood pressure transducer (model TAP20-C10; Data Sciences International, St. Paul, MN), securing the device body in the abdominal cavity. Diastolic, systolic and mean arterial pressures, as well as heart rate, were collected every 10 minutes continuously for 3 weeks, beginning immediately after implantation. At the end of 3 weeks, 3 consecutive 28-hour periods were averaged from each mouse, and a group mean was calculated. Rate-pressure product (mVO_2), an indicator of myocardial oxygen consumption, was calculated from systolic pressure × heart rate.

Isometric force measurements

Vascular rings (2-3 mm in length) with or without endothelium were mounted in a myograph system (Danish Myo Technology A/S, Aarhus, Denmark) and bathed with warmed (37°C), aerated (95% O_2/5% CO_2) physiological salt solution (PSS, mmol/L: NaCl 130, KCl 4.7, $KHPO_4$ 1.18, $MgSO_4$ 1.17, $CaCl_2$ 1.6, $NaHCO_3$ 14.9, dextrose 5.5, $CaNa_2$ EDTA 0.03). Carotid rings were denuded of endothelium using a human hair, and thoracic aortic rings were denuded of endothelium by perfusing the rings with 100 μL of 0.1% triton in PBS (15). Carotid rings were set at 250 mg passive tension while thoracic aortic rings were set at 700mg passive tension. These passive tensions were chosen based on previous studies in the carotid artery (16) and thoracic aorta (17). Arterial preparations were equilibrated for 1 hour with washes every 20 minutes. Prior to experimental protocols, rings were subjected to a wake-up protocol consisting of 2 consecutive contractions with KPSS (mmol/L: NaCl 14.7, KCl 100, $KHPO_4$ 1.18, $MgSO_4$ 1.17, $CaCl_2$ 1.6, $NaHCO_3$ 14.9, dextrose 5.5, $CaNa_2$ EDTA 0.03) and phenylephrine (PE; 10^{-6} mol/L) with washes in between each KPSS contraction. After the PE contraction reached a plateau in the thoracic aortas, endothelial integrity was tested with 10^{-5} mol/L acetylcholine (Ach). The carotid rings were not exposed to Ach during the wake up protocol, because previous exposure of the arterial preparations to Ach or SNP desensitizes the preparations to endothelium-dependent contractions (18).

Experimental protocols

Endothelium-dependent contraction—The carotid arteries were used to evaluate endothelium-dependent contractions since aortas do not have as robust an endothelium-dependent contraction as carotids (19). All equilibration and reactivity in the carotid rings (KPSS and Ach-induced contractions) were performed in the presence of 3×10^{-4} mol/L N_{ω}-nitro-$_L$-arginine (LNNA). After the wake-up protocol was performed, the PE contraction was washed out. Because of the biphasic nature of the Ach-mediated contraction, only a single concentration of Ach (10^{-5} mol/L) was used on the arterial preparations (19). A total of 10 mice were used for reactivity in the carotid arteries.

Vascular smooth muscle contractility—The thoracic aortas were used to evaluate vascular smooth muscle reactivity in endothelium intact rings in the presence or absence of 3×10^{-4} mol/L LNNA, or endothelium-denuded rings. After the wake-up protocol, cumulative concentrations of PE (10^{-9} mol/L to 10^{-5} mol/L), serotonin (5HT; 10^{-9} mol/L to 10^{-5} mol/L), or the PGH_2/TxA_2 (TP) receptor agonist, U46619 (10^{-11} mol/L to 3×10^{-7} mol/L) were added to the bath to establish a concentration-response curve. Contractions to PE, 5HT or U46619 were expressed as a percent of the second KPSS contraction. 5HT and U46619 reactivity were performed in a group of aortas different from those used for PE.

Endothelium-dependent and endothelium-independent relaxation—In rings of thoracic aorta in which a PE concentration response was performed, the PE contraction was washed out, and the PE EC_{80} was calculated for each individual ring. The individual PE EC_{80} values were used to contract the appropriate rings and allowed to reach a stable plateau. Ach (10^{-10} mol/L to 10^{-5} mol/L), ionomycin (10^{-10} mol/L to 3×10^{-7} mol/L) or sodium nitroprusside (SNP; 10^{-11} mol/L to 10^{-6} mol/L) was added cumulatively to the bath to examine endothelium-dependent (Ach and ionomycin) or – independent (SNP) relaxation. Ach, ionomycin, and SNP relaxation were expressed as a percent of the PE EC_{80} contraction. Ach and SNP reactivity were performed in the same rings, while ionomycin reactivity was performed in separate rings that did not receive Ach or SNP. Separate reactivity to all agonists also was performed in the presence of LNNA (10^{-4} mol/L). PE, Ach, and SNP reactivity were also performed again in separate rings denuded of endothelium.

Chemicals

PE, 5HT, Ach, SNP, LNNA, triton and all salts for PSS were purchased from Sigma Chemical Co. (St. Louis, MO). U46619 was purchased from Cayman Chemical (Ann Arbor, MI). Ionomycin was purchased from Calbiochem (La Jolla, CA).

Data and Statistical Analysis

Agonist EC_{50} values were calculated with a nonlinear regression analysis with the algorithm [effect = maximum response/1 + (EC_{50}/agonist concentration)] in the computer program GraphPad Prism (San Diego, CA). Hill slope values were also derived from GraphPad Prism. The PE EC_{80} values were calculated from the equation, $\log EC_{50} = \log EC_F - (1/\text{HillSlope}) * \log (F/[100-F])$, where F = 80. Data were expressed as mean ± SEM. Blood pressures, heart-rate, and rate-pressure products were analyzed using two-way ANOVA. Concentration-response data were analyzed using two-way ANOVA to compare the concentration-response curves between groups. The Bonferonni post hoc test was used to assess differences at individual points on the concentration-response curves if the two-way ANOVA comparison between curves was $p < 0.05$. One-way ANOVA was used to evaluate differences between groups in endothelium-dependent contractions. Differences in KPSS contractions, EC_{50}, and E_{max} between 2 groups were analyzed by student t-test. A $p < 0.05$ was considered statistically significant.

Results

Blood pressure and heart rate in wildtype (WT) and *Gla* knockout (*Gla* -/0) mice

Blood pressure and heart rate measured in WT and *Gla* -/0 are illustrated in Figure 1 and Figure 2. Diastolic (Figure 1a), systolic (Figure 1b) and mean arterial pressure (Figure 1c) fluctuated due to circadian rhythms but did not differ between the 2 groups over the 28 hour period measured, suggesting the *Gla* -/0 mice were not hypertensive. Heart rate (Figure 2) also fluctuated through the 28 hour period due to circadian rhythms. The heart rates in *Gla* -/0 mice were higher, but not statistically significant, compared to WT mice during the dark cycle. The rate-pressure product (mVO_2), a calculated index of myocardial oxygen consumption (Figure 2b) was also higher, but not significantly different in the *Gla* -/0 mice compared to WT mice during the dark cycle, suggesting the hearts in *Gla* -/0 mice may be working harder to maintain perfusion pressure.

Vascular contractility with phenylephrine, serotonin, and U46619

Phenylephrine (PE)—The vascular contraction mediated by 100 mmol/L KPSS was equivalent in aortas from wildtype (*Gla* +/0) and *Gla* knockout (*Gla* -/0) mice (1708 ± 107

mg; n=16 vs. 1496 ± 93 mg; n=16, respectively; $p > 0.05$). KPSS contractions, in the presence of N_{ω}-nitro-$_L$-arginine (LNNA), were 2078 ± 99 mg (n=12) for *Gla* +/0 versus 2056 ± 93 mg (n=13) for *Gla* -/0 ($p > 0.05$). After endothelial denudation, KPSS contractions were 1065 ± 123 mg (n=5) for *Gla* +/0 versus 1007 ± 118 mg (n=5) for *Gla* -/0 ($p > 0.05$).

PE caused a concentration-dependent contraction in isolated endothelium-intact aortic rings from both *Gla* +/0 and *Gla* -/0 mice (figure 3). PE contractility in untreated, endothelium-intact vessels (figure 3a) was approximately 2-fold less sensitive in aortas from *Gla* -/0 mice compared to *Gla* +/0 (Table 1). In addition, maximal contraction (E_{max}) to PE in aortas from *Gla* -/0 mice was significantly less (E_{max} = 92.9 ± 3.7 %) compared to that in aortas from *Gla* +/0 mice (E_{max} = 107.9 ± 4.0 %; $p < 0.05$). PE contractility in the presence of LNNA (figure 3b) was still less sensitive (~1.6-fold less) in aortas from *Gla* -/0 mice compared to *Gla* +/0 mice (Table 2) while maximal contraction to PE were not different in the presence of LNNA (E_{max} = 122.5 ± 3.1 % for *Gla* +/0 vs. 121.1 ± 3.6 % for *Gla* -/0; $p > 0.05$). Figure 3c illustrates PE reactivity in endothelium-denuded aortas from *Gla* +/0 and *Gla* -/0 mice. The PE-induced contractions were equivalent in aortas from *Gla* +/0 and *Gla* -/0 mice as demonstrated by similar log EC_{50} values (Table 3) as well as equivalent E_{max} values (189.9 ± 22.6 % vs. 198.0 ± 24.8 %, respectively; $p > 0.05$).

Serotonin (5HT)—The vascular contraction mediated by 100 mmol/L KPSS for 5HT and U46619 reactivity did not differ between endothelium-intact rings from *Gla* +/0 and *Gla* -/0 mice (1225 ± 109 mg; n=8 vs. 1241 ± 101 mg; n=8, respectively; $p > 0.05$). KPSS contractions, in the presence of LNNA or endothelium denudation (-ENDO), also did not differ between *Gla* +/0 and *Gla* -/0 (LNNA: *Gla* +/0 = 1414 ± 60 mg; n=6 vs. *Gla* -/0 = 1455 ± 73 mg; n=6, $p > 0.05$; -ENDO: *Gla* +/0 = 1064 ± 76 mg; n=6 vs. *Gla* -/0 = 1043 ± 82 mg; n=5, $p > 0.05$).

5HT contractility occurred in a concentration-dependent manner, as illustrated in figure 4. Similar to PE, 5HT contractility in endothelium-intact aortic rings (figure 4a) from *Gla* -/0 mice were significantly less sensitive to the contractility in aortas from *Gla* +/0 (Table 1). Maximal contraction (E_{max}) to 5HT in aortas from *Gla* -/0 mice also was significantly less (E_{max} = 119.4 ± 5.7 %) compared to that in aortas from *Gla* +/0 mice (E_{max} = 138.3 ± 2.9 %; $p < 0.05$). In the presence of LNNA (figure 4b), the difference in E_{max} was no longer significant (*Gla* +/0 + LNNA E_{max} = 116.3 ± 1.7 % vs. *Gla* -/0 + LNNA E_{max} = 108.1 ± 5.3 %; $p > 0.05$), but the difference in sensitivity was maintained (Table 2). Similarly, when endothelium was removed (figure 4c), 5HT E_{max} was no longer significant (*Gla* +/0 -ENDO E_{max} = 161.1 ± 5.9 % vs. *Gla* -/0 -ENDO E_{max} = 162.8 ± 12.2 %; $p > 0.05$), but unlike PE, the 5HT log EC_{50} in *Gla* -/0 was still less sensitive than the 5HT log EC_{50} in *Gla* +/0 (Table 3).

The TP receptor agonist, U46619—The 3rd vasopressor, U46619, also caused concentration-dependent contractions in the aortic rings from both *Gla* +/0 and *Gla* -/0 mice (figure 5). U46619 U46619 E_{max} contractility, however, did not differ between *Gla* +/0 and *Gla* -/0, regardless of whether endothelium was present (figure 5a: *Gla* +/0 E_{max} = 177.9 ± 5.3 % vs. *Gla* -/0 E_{max} = 169.4 ± 7.0 %; $p > 0.05$), LNNA was present (figure 5b: *Gla* +/0 + LNNA E_{max} = 132.7 ± 4.0 % vs. *Gla* -/0 + LNNA E_{max} = 142.4 ± 4.7 %; $p > 0.05$) or endothelium was absent (figure 5c: *Gla* +/0 -ENDO E_{max} = 193.0 ± 11.1 % vs. *Gla* -/0 + LNNA E_{max} = 211.5 ± 19.9 %; $p > 0.05$). The EC_{50} for *Gla* -/0 with endothelium was minimally different, yet still statistically significant, compared to *Gla* +/0 with endothelium (Table 1). Likewise was observed when U46619 contractility was performed in the presence of LNNA (Table 2). Removing the endothelium, however, resulted in similar EC_{50} values for both *Gla* +/0 and *Gla* -/0 (Table 3).

Endothelium-dependent contraction with acetylcholine (Ach)

Endothelium-dependent contraction to Ach was examined in isolated carotid arteries from *Gla* +/0 and *Gla* -/0 mice (figure 6). The carotid arteries were used because they display a much more robust endothelium-dependent contraction to Ach compared to the aorta (19) KPSS contractions in endothelium-intact carotid rings from *Gla* +/0 and *Gla* -/0 mice were equivalent (*Gla* +/0 = 514 ± 56 mg, n=5; *Gla* -/0 = 490 ± 46 mg, n=5). In carotid arteries at baseline resting conditions, Ach (10^{-5} mol/L), in the presence of 3×10^{-4} mol/L LNNA, caused a contraction that was absent in the endothelium-denuded arteries. However, the endothelium-dependent contraction elicited by Ach was significantly less in the carotids from *Gla* -/0 mice (~ 49% less) compared to *Gla* +/0 mice.

Receptor-mediated endothelium-dependent relaxation with acetylcholine (Ach)

Endothelium-dependent relaxation to Ach also was examined in isolated aortas from *Gla* +/0 and *Gla* -/0 mice pre-contracted with a PE EC_{80} calculated for each ring after the PE concentration response. Aortic rings from *Gla* -/0 mice relaxed significantly less (E_{max} = 62.5 ± 6.3 %) compared to rings from *Gla* +/0 mice (E_{max} = 83.3 ± 2.9 %) (figure 7a). Ach responses are eNOS and endothelium dependent, since both LNNA (figure 7b) and endothelium denudation (figure 7c) prevented any Ach-mediated relaxation in the pre-contracted aortic rings from *Gla* +/0 and *Gla* -/0 mice.

Non receptor-mediated endothelium-dependent relaxation with ionomycin

The calcium ionophore, ionomycin, was used to induce non-receptor mediated eNOS-dependent relaxations in endothelium-intact vessels pre-contracted with an EC_{80} of PE, as illustrated in figure 8. Ionomycin-induced relaxation (figure 8a) did not differ between vessels from *Gla* +/0 (log EC_{50} = -7.98 ± 0.03 mol/L and E_{max} = 95.5 ± 2.1 %) and *Gla* -/0 mice (log EC_{50} = -8.01 ± 0.02 mol/L and E_{max} = 94.5 ± 1.7 %). Ionomycin caused a slight relaxation in the pre-contracted endothelium-intact aortic rings from *Gla* +/0 and *Gla* -/0 mice incubated with LNNA (figure 8b), but no differences existed between the 2 groups in sensitivity or maximal response in the presence of LNNA.

Endothelium-independent relaxation with sodium nitroprusside (SNP)

SNP mediated a concentration-dependent, endothelium-independent relaxation in isolated thoracic aortas from *Gla* +/0 and *Gla* -/0 mice. In the presence of endothelium, the SNP-induced relaxation was less sensitive in the vessels from *Gla* -/0 mice compared to vessels from *Gla* +/0 mice (Table 1). Vessels exposed to the NOS inhibitor, LNNA, were significantly more sensitive to SNP compared to their respective vessels with intact endothelium without LNNA (Table 2). Similarly, aortas denuded of endothelium (-ENDO) also displayed increased sensitivity to SNP, compared to their untreated, endothelium-intact counterparts (Table 3) and were similar in sensitivity to LNNA-treated vessels.

Discussion

Fabry disease has a complex cardiovascular phenotype. Premature mortality is more often the result of stroke and myocardial infarctions (20). Informative clinical studies in Fabry disease patients have documented both macrovascular and microvascular dysfunction, suggesting that the pathophysiology may be highly complex (21,22). The α-galactosidase A knockout mouse (*Gla* -/0) provides a potentially useful tool to study these cardiovascular phenomenon. Indeed, our group has reported that these mice are more susceptible to oxidant induced thrombosis and accelerated atherogenesis (7,11). In this study we used this model to ascertain the role of the endothelium in large vessel reactivity.

We report several novel observations in this *Gla* -/0 murine model of Fabry disease. First, abnormal vasopressor contractility to phenylephrine (PE) and serotonin (5HT) in the *Gla* -/0 aortas are less sensitive than that in the wildtype (*Gla* +/0) aortas but are normal to a thromboxane A_2/prostaglandin H_2 (TP) receptor agonist or when the endothelium is removed. Second, endothelium-dependent contraction is significantly less in the *Gla* -/0 carotid arteries compared to *Gla* +/0 carotid arteries. Third, impaired endothelium-dependent relaxation is not observed when a calcium ionophore is used to mediate endothelium-dependent relaxation. These observations are important because the defects observed in this murine model of Fabry disease demonstrate a complexity of the reactivity that can be attributed entirely to the endothelium, even though elevated Gb3 levels occur in the other vascular cell-types (7,13).

In many vascular diseases such as hypertension and diabetes, vascular smooth muscle (VSM) vasopressor sensitivity is increased, while endothelium-dependent relaxation is diminished (23-26). Our data were surprising because abhorrent endothelium-dependent relaxation was observed but a concomitant increased sensitivity to vasopressor activity was absent, as illustrated by decreased sensitivity to PE or 5HT, in the presence of endothelium, while TP receptor –mediated VSM contraction with U46619 was similar in *Gla* -/0 mice compared to *Gla* +/0 mice.

How this anomaly developed in our mouse model of Fabry disease is unclear, but we speculate on several mechanisms that may partially explain our observations. If basal nitric oxide (NO) production is higher in the *Gla* -/0 mice, then VSM contraction would be inhibited. Additionally, if agonist-stimulated NO production is less in the *Gla* -/0 mice, for whatever reason, endothelium-dependent relaxation also would be inhibited or diminished. However, persistence in the decreased sensitivity to vasopressor in the presence of LNNA does not support that hypothesis, suggesting that the endothelium may be producing another factor to cause endothelium-dependent relaxation after stimulation with acetylcholine (Ach). Prostaglandin I_2, which mediates endothelium-dependent relaxation by activation of cAMP in vascular smooth muscle (27), is a potential mechanism by which our anomalous reactivity may be occurring. However, whether cyclooxygenase-derived products have any role in the vascular dysfunction or are in some way regulated by glycosphingolipids is yet to be determined.

Alternatively, on a more cellular level, in cells subjected to pathologically increased levels of Gb3, excess Gb3 content may be present in compartments outside of the lysosome, including lipid rafts or caveolae. Recently, we reported that Gb3 and other globo series GSLs are concentrated higher in caveolae from *Gla* -/0 endothelial cells compared to *Gla* +/0 endothelial cells (28). These changes in GSLs increase as a function of age and are accompanied by corresponding decreases in cholesterol. Additionally, GSL concentrations in caveolae change dynamically after endothelial cells are exposed to recombinant α-galactosidase A or the glucosylceramide synthase inhibitor D-*threo*-ethylenedioxyphenyl-2-palmitoylamino-3-pyrillidino-propanol. Modulation of cellular GSL content regulates bradykinin-induced src kinase and phospholipase C_γ activation (29,30). Conversely, increased Gb3 accumulation in the endothelial cells may inhibit receptor-induced signaling responsible for activation of endothelial nitric oxide synthase (eNOS). Our endothelium-dependent relaxation with the calcium ionophore, ionomycin, support this potential mechanism, since the ionophore relaxation is normal in the aortas from the *Gla* -/0 mice compared to the *Gla* +/0 mice, while the receptor-induced endothelium-dependent relaxation to Ach is attenuated in the aortas from the *Gla* -/0 mice.

Since these caveolar domains are enriched with and regulate eNOS, accumulated caveolar GSL associated with Fabry disease may conceivably alter eNOS activation by one of 2

mechanisms. First, eNOS and caveolin interactions are affected by excess Gb3 or a related sphingolipid or, alternatively, by secondary changes in other raft associated lipids. Second, receptor coupling to downstream mediators may be affected, since sphingolipid, as well as cholesterol, content in lipid rafts or caveolae can modulate the fluidity of these signaling "hotspots" (31). Our data appear to support the latter mechanism since eNOS activation independent of a receptor, is normal, suggesting that any interactions between eNOS and caveolin-1 are not affected by increased caveolar Gb3 content. Further studies are needed, however, to demonstrate that receptor coupling is affected by excess endothelial Gb3 in this mouse model of Fabry disease. Our endothelium-dependent contraction data and our endothelium-dependent relaxation data combined, however, are consistent with the hypothesis that receptor coupling is affected in this mouse model of Fabry disease, since both are attenuated in the *Gla* -/0 mice, especially since endothelium-dependent contractions, in the face of endothelial dysfunction, should be augmented.

Our data indicate that, whatever the mechanism might be, our changes in vascular function in the *Gla* -/0 mice are localized to the endothelium. This conclusion is supported by 2 main observations. First, most of the vascular contractility to vasopressor is close to normal after endothelium denudation. Second, endothelium-dependent contraction is significantly attenuated in the *Gla* -/0 mice, a phenomenon which is due to the paracrine release of a TP receptor agonist from the endothelium (32). Direct stimulation of VSM contraction with the TP receptor agonist, U46619, however, did not reveal any differences between *Gla* -/0 and *Gla* +/0.

In conclusion, we demonstrate that the vasculopathy associated with *Gla* -/0 mice occurs at a younger age than previously reported (13), and that the early vasculopathy are localized to the endothelium. Importantly, the vaculopathy reported here may be a result of impaired receptor signaling rather than impaired eNOS activity. These findings provide insight into how early vaculopathy may develop in Fabry disease, but they also suggest that glycosphingolipid metabolism may play a subtle, yet significant role in the regulation of receptor-mediated signaling.

Acknowledgments

This work was supported by NIH grant 5RO1DK055823-06. Some of this work was reported at the International Society of Nephrology Forefronts in Nephrology Conference on Endothelial Biology, in March, 2006.

References

1. Kint JA. The enzyme defect in Fabry's disease. Nature. 1970; 227:1173. [PubMed: 5451124]
2. Kint JA. Fabry's disease: alpha-galactosidase deficiency. Science. 1970; 167:1268–9. [PubMed: 5411915]
3. Sweeley CC, Klionsky B. Fabry's Disease: Classification as a Sphingolipidosis and Partial Characterization of a Novel Glycolipid. J Biol Chem. 1963; 238:3148–50. [PubMed: 14081947]
4. Brady RO, Gal AE, Bradley RM, Martensson E, Warshaw AL, Laster L. Enzymatic defect in Fabry's disease. Ceramidetrihexosidase deficiency. N Engl J Med. 1967; 276:1163–7. [PubMed: 6023233]
5. Desnick, RJ.; Ioannou, YA.; Eng, CM. a-Galactosidase A Deficiency: Fabry Disease. In: Scriver, CR.; Beaudet, AL.; Sly, WS.; Valle, D., editors. The Metabolic and Molecular Bases of Inherited Disease. 8th. McGraw-Hill; New York: 2001.
6. Desnick RJ, Banikazemi M, Wasserstein M. Enzyme replacement therapy for Fabry disease, an inherited nephropathy. Clin Nephrol. 2002; 57:1–8. [PubMed: 11837797]
7. Eitzman DT, Bodary PF, Shen Y, et al. Fabry disease in mice is associated with age-dependent susceptibility to vascular thrombosis. J Am Soc Nephrol. 2003; 14:298–302. [PubMed: 12538729]

8. Shu L, Murphy HS, Cooling L, Shayman JA. An in vitro model of Fabry disease. J Am Soc Nephrol. 2005; 16:2636–45. [PubMed: 16033856]
9. Ohshima T, Murray GJ, Swaim WD, et al. alpha-Galactosidase A deficient mice: a model of Fabry disease. Proc Natl Acad Sci U S A. 1997; 94:2540–4. [PubMed: 9122231]
10. Shen Y, Bodary PF, Vargas FB, et al. Alpha-galactosidase A deficiency leads to increased tissue fibrin deposition and thrombosis in mice homozygous for the factor V Leiden mutation. Stroke. 2006; 37:1106–8. [PubMed: 16514103]
11. Bodary PF, Shen Y, Vargas FB, et al. Alpha-galactosidase A deficiency accelerates atherosclerosis in mice with apolipoprotein E deficiency. Circulation. 2005; 111:629–32. [PubMed: 15668341]
12. Moore DF, Gelderman MP, Fuhrmann SR, Schiffmann R, Brady RO, Goldin E. Fabry disease and vascular risk factors: future strategies for patient-based studies and the knockout murine model. Acta Paediatr Suppl. 2006; 95:69–71. [PubMed: 16720469]
13. Heare T, Alp NJ, Priestman DA, et al. Severe endothelial dysfunction in the aorta of a mouse model of Fabry disease; partial prevention by N-butyldeoxynojirimycin treatment. J Inherit Metab Dis. 2007; 30:79–87. [PubMed: 17189993]
14. Whitesall SE, Hoff JB, Vollmer AP, D'Alecy LG. Comparison of simultaneous measurement of mouse systolic arterial blood pressure by radiotelemetry and tail-cuff methods. Am J Physiol Heart Circ Physiol. 2004; 286:H2408–15. [PubMed: 14962829]
15. Tang EH, Ku DD, Tipoe GL, Feletou M, Man RY, Vanhoutte PM. Endothelium-dependent contractions occur in the aorta of wild-type and COX2-/- knockout but not COX1-/- knockout mice. J Cardiovasc Pharmacol. 2005; 46:761–5. [PubMed: 16306799]
16. Faraci FM, Sigmund CD, Shesely EG, Maeda N, Heistad DD. Responses of carotid artery in mice deficient in expression of the gene for endothelial NO synthase. Am J Physiol. 1998; 274:H564–70. [PubMed: 9486260]
17. Park JL, Loberg RD, Duquaine D, et al. GLUT4 facilitative glucose transporter specifically and differentially contributes to agonist-induced vascular reactivity in mouse aorta. Arterioscler Thromb Vasc Biol. 2005; 25:1596–602. [PubMed: 15890973]
18. Tang EH, Feletou M, Huang Y, Man RY, Vanhoutte PM. Acetylcholine and sodium nitroprusside cause long-term inhibition of EDCF-mediated contractions. Am J Physiol Heart Circ Physiol. 2005; 289:H2434–40. [PubMed: 16040712]
19. Zhou Y, Varadharaj S, Zhao X, Parinandi N, Flavahan NA, Zweier JL. Acetylcholine causes endothelium-dependent contraction of mouse arteries. Am J Physiol Heart Circ Physiol. 2005; 289:H1027–32. [PubMed: 15879486]
20. Shayman, JA.; Killen, PD. Fabry Disease. In: Mount, DB.; Pollak, MJ., editors. Molecular and Genetic Basis of Renal Disease. Vol. Ch. 13. Saunders/Elsevier; Philadelphia: 2008.
21. Elliott PM, Kindler H, Shah JS, et al. Coronary microvascular dysfunction in male patients with Anderson-Fabry disease and the effect of treatment with alpha galactosidase A. Heart. 2006; 92:357–60. [PubMed: 16085718]
22. Moore DF, Kaneski CR, Askari H, Schiffmann R. The cerebral vasculopathy of Fabry disease. J Neurol Sci. 2007; 257:258–63. [PubMed: 17362993]
23. Guo Z, Su W, Allen S, et al. COX-2 up-regulation and vascular smooth muscle contractile hyperreactivity in spontaneous diabetic db/db mice. Cardiovasc Res. 2005; 67:723–35. [PubMed: 15885672]
24. Linder AE, Weber DS, Whitesall SE, D'Alecy LG, Webb RC. Altered vascular reactivity in mice made hypertensive by nitric oxide synthase inhibition. J Cardiovasc Pharmacol. 2005; 46:438–44. [PubMed: 16160594]
25. Pannirselvam M, Verma S, Anderson TJ, Triggle CR. Cellular basis of endothelial dysfunction in small mesenteric arteries from spontaneously diabetic (db/db -/-) mice: role of decreased tetrahydrobiopterin bioavailability. Br J Pharmacol. 2002; 136:255–63. [PubMed: 12010774]
26. Pannirselvam M, Wiehler WB, Anderson T, Triggle CR. Enhanced vascular reactivity of small mesenteric arteries from diabetic mice is associated with enhanced oxidative stress and cyclooxygenase products. Br J Pharmacol. 2005; 144:953–60. [PubMed: 15685205]
27. Shepherd JT, Katusic ZS. Endothelium-derived vasoactive factors: I. Endothelium-dependent relaxation. Hypertension. 1991; 18:III76–85. [PubMed: 1937690]

28. Shu L, Shayman JA. Caveolin-associated accumulation of globotriaosylceramide in the vascular endothelium of alpha-galactosidase A null mice. J Biol Chem. 2007; 282:20960–7. [PubMed: 17535804]

29. Shu L, Lee L, Shayman JA. Regulation of phospholipase C-gamma activity by glycosphingolipids. J Biol Chem. 2002; 277:18447–53. [PubMed: 11886852]

30. Shu L, Shayman JA. Src kinase mediates the regulation of phospholipase C-gamma activity by glycosphingolipids. J Biol Chem. 2003; 278:31419–25. [PubMed: 12771140]

31. Brown DA, London E. Structure and function of sphingolipid- and cholesterol-rich membrane rafts. J Biol Chem. 2000; 275:17221–4. [PubMed: 10770957]

32. Vanhoutte PM, Feletou M, Taddei S. Endothelium-dependent contractions in hypertension. Br J Pharmacol. 2005; 144:449–58. [PubMed: 15655530]

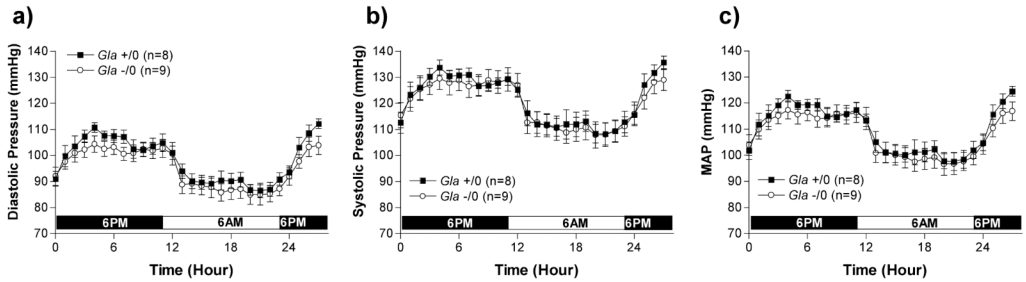

Figure 1.

a) Conscious diastolic, **b)** systolic, and **c)** mean arterial, blood pressures (mmHg) measured during a 28-hour light-dark cycle by telemetry in wildtype (*Gla +/0*) or *Gla* knockout (*Gla -/0*) mice. p>0.05 by two-way ANOVA.

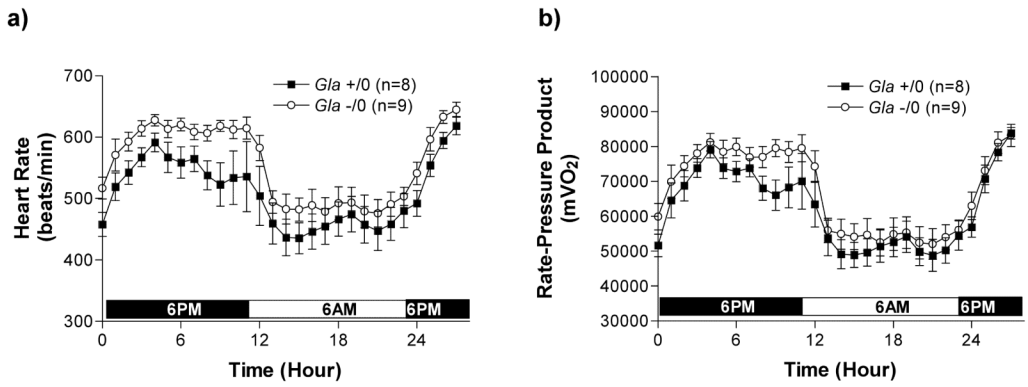

Figure 2.

a) Heart rate (beats/min), and calculated myocardial oxygen consumption (mVO_2) or **b)** Rate-Pressure Product obtained from measurements derived from a telemetric blood pressure transducer. $p>0.05$ by two-way ANOVA.

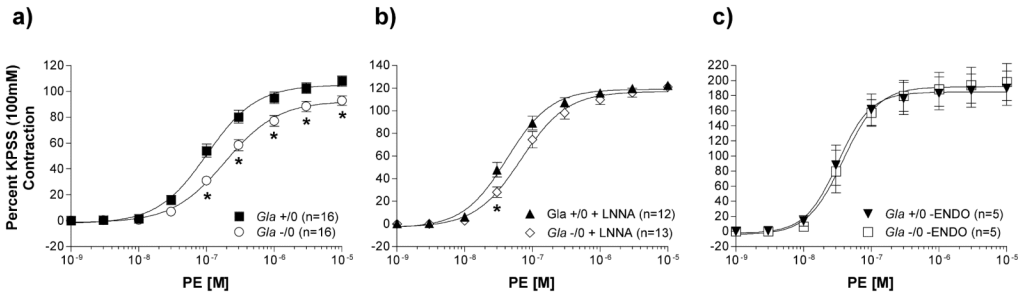

Figure 3.

Phenylephrine (PE)-mediated vascular contraction in endothelium-intact mouse aortic rings from wildtype (*Gla +/0*) or *Gla* knockout (*Gla* -/0) mice **a)** alone without any pharmacological intervention, **b)** in the presence of 10^{-4} mol/L N_{ω}-nitro-$_{L}$-arginine (LNNA), or **c)** with endothelium denuded. Data are expressed as a percentage of the contraction elicited by a 100 mmol/L KCl-containing physiological salt solution. * = $p<0.05$ compared to *Gla* +/0 by two-way ANOVA followed by Bonferonni post hoc test.

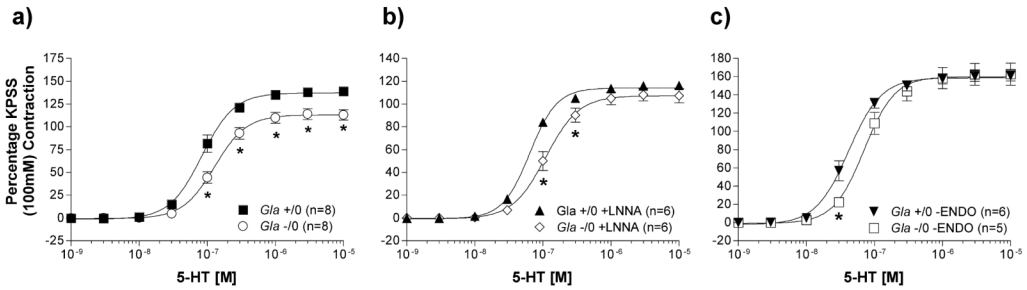

Figure 4.

Serotonin (5HT)-mediated vascular contraction in endothelium-intact mouse aortic rings from wildtype (*Gla +/0*) or *Gla* knockout (*Gla* -/0) mice **a)** alone without any pharmacological intervention, **b)** in the presence of 10^{-4} mol/L N_{ω}-nitro-$_{L}$-arginine (LNNA), or **c)** with endothelium denuded. Data are expressed as a percentage of the contraction elicited by a 100 mmol/L KCl-containing physiological salt solution. * = $p<0.05$ compared to *Gla* +/0 by two-way ANOVA followed by Bonferonni post hoc test.

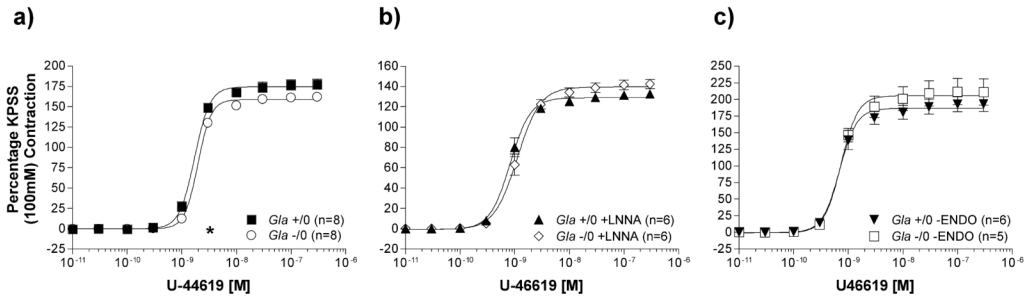

Figure 5.

The thromboxane A_2/prostaglandin H_2 (TP) receptor agonist, U46619, mediated vascular contraction in endothelium-intact mouse aortic rings from wildtype (*Gla +/0*) or *Gla* knockout (*Gla* -/0) mice **a)** alone without any pharmacological intervention, **b)** in the presence of 10^{-4} mol/L N_{ω}-nitro-$_L$-arginine (LNNA), or **c)** with endothelium denuded. Data are expressed as a percentage of the contraction elicited by a 100 mmol/L KCl-containing physiological salt solution. * = $p<0.05$ compared to *Gla* +/0 by two-way ANOVA followed by Bonferonni post hoc test.

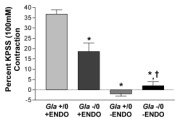

Figure 6.

Endothelium-dependent contraction mediated by 10^{-5} mol/L acetylcholine (Ach) in endothelium-intact and endothelium-denuded (-ENDO) mouse carotid artery rings from wildtype (*Gla +/0*) or *Gla* knockout (*Gla* -/0) mice in the presence of 3×10^{-4} mol/L N_{ω}-nitro-$_L$-arginine (LNNA). * = $p<0.05$ compared to *Gla* +/0 and † = $p<0.05$ compared to *Gla* +/0 –ENDO by one-way ANOVA; n=5 in each group.

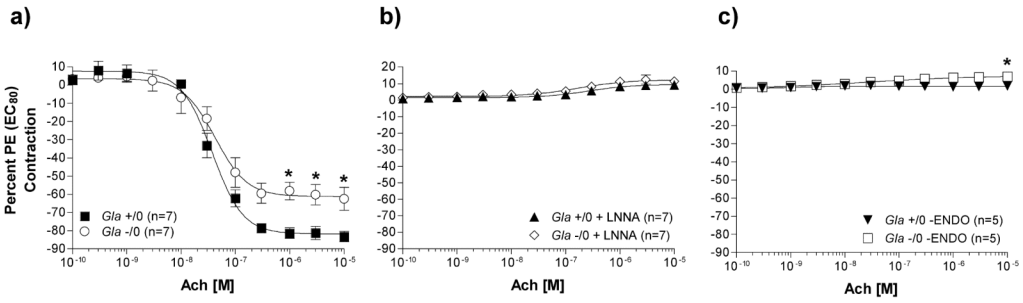

Figure 7.

Acetylcholine (Ach)-mediated endothelium-dependent relaxation in endothelium-intact mouse aortic rings from wildtype (*Gla +/0*) or *Gla* knockout (*Gla* -/0) mice pre-contracted with an EC_{80} concentration of PE **a)** alone without any pharmacological intervention, **b)** in the presence of 10^{-4} mol/L N_{ω}-nitro-$_{L}$-arginine (LNNA), or **c)** with endothelium denuded. Data are expressed as a percentage of the contraction elicited by PE EC_{80}. * = $p<0.05$ compared to *Gla* +/0 by two-way ANOVA followed by Bonferonni post hoc test.

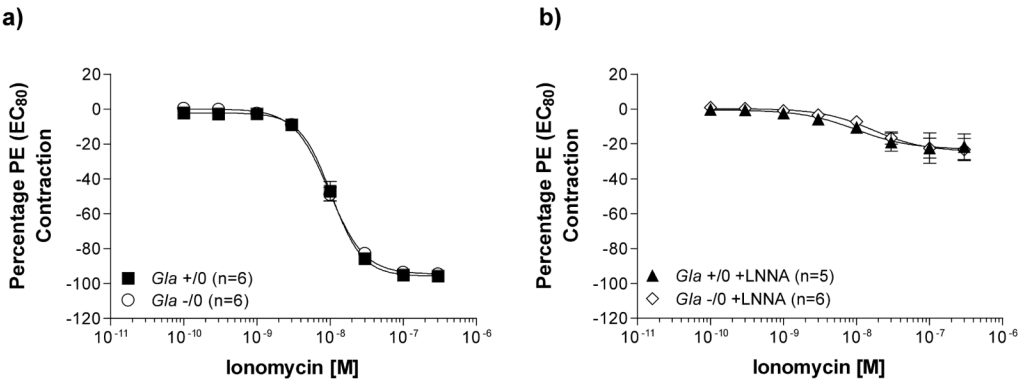

Figure 8.

Ionomycin-induced eNOS-dependent relaxation in endothelium-intact mouse aortic rings from wildtype (*Gla +/0*) or *Gla* knockout (*Gla* -/0) mice pre-contracted with an EC_{80} concentration of PE **a)** alone without any pharmacological intervention or **b)** in the presence of 10^{-4} mol/L N_{ω}-nitro-$_{L}$-arginine (LNNA). Data are expressed as a percentage of the contraction elicited by PE EC_{80}. $p>0.05$ by two-way ANOVA in all figures.

Table 1

Potency of agonists in vascular reactivity of thoracic aortas with endothelium intact from wildtype (*Gla* +/0) or *Gla* knockout (*Gla* -/0) mice. Data are reported as mean ± SEM for the number of animals in parentheses. The EC_{50} values are expressed as the −log EC_{50} for each agonist. * = $p<0.05$ compared to *Gla* +/0 by the Student *t* test.

	-log EC_{50} [M]	
Agonist	***Gla* +/0 (+ENDO)**	***Gla* -/0 (+ENDO)**
PE	6.99 ± 0.05 (16)	6.72 ± 0.05 (16) *
5HT	7.08 ± 0.03 (8)	6.89 ± 0.04 (8) *
U46619	8.77 ± 0.02 (8)	8.70 ± 0.02 (8) *
Ach	7.43 ± 0.05 (7)	7.37 ± 0.10 (7)
Ionomycin	7.98 ± 0.03 (6)	8.01 ± 0.02 (6)
SNP	8.27 ± 0.10 (7)	7.93 ± 0.05 (7) *

Table 2

Potency of agonists in vascular reactivity of thoracic aortas with endothelium intact, in the presence of 3×10^{-4} mol/L N_{ω}-nitro-$_L$-arginine (LNNA) from wildtype (*Gla* +/0) or *Gla* knockout (*Gla* -/0) mice. Data are reported as mean ± SEM for the number of animals in parentheses. The EC_{50} values are expressed as the −log EC_{50} for each agonist. * = $p<0.05$ compared to *Gla* +/0 by the Student *t* test.

	-log EC_{50} [M]	
Agonist	***Gla* +/0 (+LNNA)**	***Gla* -/0 (+LNNA)**
PE	7.37 ± 0.04 (12)	7.17 ± 0.05 (13) *
5HT	7.19 ± 0.02 (6)	6.96 ± 0.04 (6) *
U46619	9.08 ± 0.03 (6)	8.95 ± 0.03 (6) *
Ach	6.57 ± 0.20 (7)	6.76 ± 0.31 (7)
Ionomycin	8.01 ± 0.31 (5)	7.77 ± 0.21 (6)
SNP	9.07 ± 0.13 (5)	9.11 ± 0.02 (5) *

Table 3

Potency of agonists in vascular reactivity of endothelium-denuded thoracic aortas from wildtype (*Gla* +/0) or *Gla* knockout (*Gla* -/0) mice. Data are reported as mean ± SEM for the number of animals in parentheses. The EC_{50} values are expressed as the −log EC_{50} for each agonist. * = $p<0.05$ compared to *Gla* +/0 by the Student *t* test.

	-log EC_{50} [M]	
Agonist	***Gla* +/0 (-ENDO)**	***Gla* -/0 (-ENDO)**
PE	7.49 ± 0.10 (5)	7.42 ± 0.10 (5)
5HT	7.38 ± 0.04 (6)	7.15 ± 0.05 (5) *
U46619	9.16 ± 0.04 (6)	9.13 ± 0.02 (5)
Ach	8.85 ± 0.95 (5)	7.57 ± 0.86 (5)
Ionomycin	N.D.	N.D.
SNP	9.07 ± 0.02 (5)	9.11 ± 0.02 (5) *